Geophys. J. Int. (2007) doi: 10.1111/j.1365-246X.2007.03353.x

Stress accumulation between volcanoes: an explanation for intra-arc earthquakes in Nicaragua?

B. Cailleau,[1] P. C. LaFemina[2*] and T. H. Dixon[2]

[1]*GFZ Potsdam, Telegrafenberg,* D-14473*, Germany. E-mail: cailleau@gfz-potsdam.de*
[2]*MGG/RSMAS, University of Miami, Rickenbacker Causeway* 4600*, Miami,* FL 33149*, USA*

Accepted 2007 January 10. Received 2007 January 10; in original form 2006 May 7

SUMMARY

Destructive upper crustal earthquakes in Central America are often located between active volcanic centres—a geometric relationship that we study using finite element Coulomb failure stress (CFS) models that incorporate the rheologically heterogeneous nature of the volcanic arc. Volcanoes are simulated as mechanically weak zones within a stronger crust. We find that deformation of the volcanic centres within a regional stress field dominated by dextral shear causes stress increases in surrounding crust, with a maximum CFS change between neighbouring volcanoes. This increase in CFS enhances the probability of fault slip on arc-normal faults that are located between volcanic centres; for example, the Tiscapa fault, which ruptured during the 1972 December 13, M_s 6.2 Managua earthquake. The amount of stress increase due to long-term (100 yr) volcano shearing is on the order of 0.1–0.6 bars, similar to values estimated for subduction zone earthquakes.

Key words: Coulomb stress, crustal deformation, finite element modelling, forearc motion.

1 INTRODUCTION

The Central American volcanic arc is volcanically and tectonically segmented, and is known for destructive upper crustal earthquakes (Stoiber & Carr 1973; Carr & Stoiber 1977; White & Harlow 1993). These earthquakes are located within 20 km of the active arc, are shallow (<25 km focal depths), have $M_s \leq 6.5$, and pose significant hazard to local population and infrastructure because of their proximity to urban areas (White & Harlow 1993) (Fig. 1b). Focal mechanisms from these earthquakes are often assumed to represent dextral strike-slip on northwest trending faults, which may accommodate forearc sliver transport resulting from oblique subduction of the Cocos Plate (White & Harlow 1993; DeMets 2001). However, the same focal mechanisms are consistent with arc-normal, northeast-striking faults, a hypothesis supported by relocated earthquakes and mapped surface ruptures (LaFemina *et al.* 2002) (Figs 1c and d). In this model, northwest-directed forearc sliver transport in Nicaragua is accommodated via block rotation, on northeast-striking, sinistral 'bookshelf' faults.

Other fault trends in the Nicaraguan arc display Holocene activity. These include north-striking normal faults that bound the Managua graben (Fig. 1d) and similarly oriented normal faults on volcanoes (Fig. 1c) (e.g. McBirney & Williams 1965; Stoiber & Carr 1973; Cowan *et al.* 2000). These faults have been attributed to NW–SE dextral shearing combined with localization by a ductile intrusion (Girard & van Wyk de Vries 2005) or volcano gravitational spreading, respectively (van Wyk de Vries & Merle 1998). North-trending volcanic vent alignments are also observed on or near volcanoes. The 30-km long Mateare fault is a major arc-parallel structure in Nicaragua, but apparently has been inactive in the last 10 000 yr (Cowan *et al.* 2000) (Fig. 1).

Although the location of seismogenic faults in Nicaragua is apparently related to the distribution of volcanic centres (White & Harlow 1993), the mechanisms by which earthquakes are localized between volcanoes remain unclear. Common understanding about the thermal or mechanical effect of crustal weakening is that weak crust is unable to sustain high stress, inhibiting great earthquakes at volcanoes. Crustal seismicity along the volcanic arc in Central America is segmented into regions of larger earthquakes between volcanoes and regions of no or smaller earthquakes near volcanoes, as expected. However, beyond this simple observation, the influence of volcanic weak zones on deformation patterns has received little attention. In this study, we investigate how volcanic centres or volcanically modified crust may affect the stress field within the surrounding crust, specifically on arc-normal strike-slip faults located between the centres (Fig. 2). Using finite element modelling, we test how mechanically weak volcanic centres embedded in stronger lithosphere behave within a regional stress field dominated by shear. Our results suggest that deformation of weak volcanic centres can cause a significant change in Coulomb failure stress (ΔCFS) on strike-slip faults located between the centres.

2 MODELLING SHEAR DEFORMATION

We use the finite element modelling program TEKTON (Melosh & Raefsky 1980) to construct simple 2-D plane stress models as

[*]Now at: Department of Geosciences, The Pennsylvania State University, University Park, PA, 16802, USA.

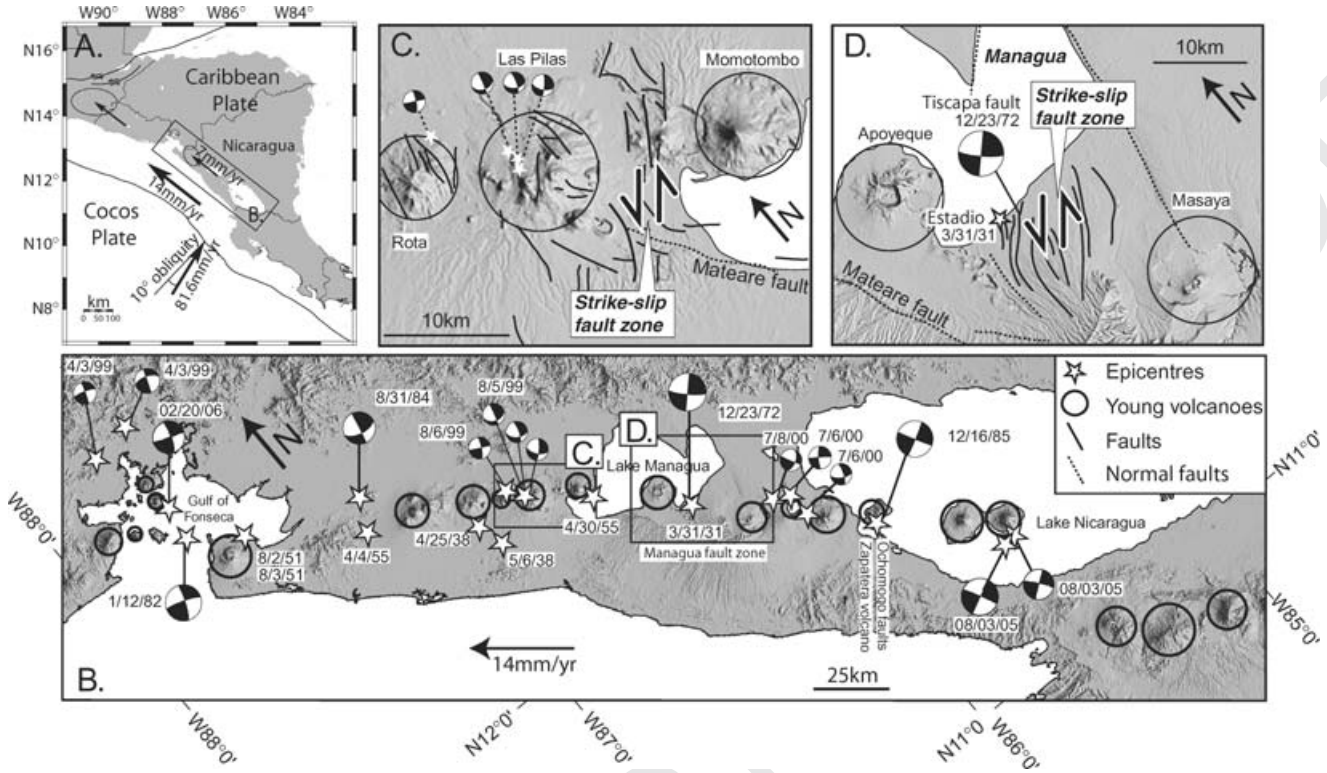

Figure 1. Tectonic and volcanic setting for Nicaragua. (A) Regional setting. The Cocos plate subducts at 10–15° obliquity, which may cause slip partitioning and forearc motion to the northwest, estimated to be $14+/-2$ mm yr^{-1} in Nicaragua (DeMets 2001). (B) Shaded relief image of the volcanic arc in Nicaragua (rotated). Black circles outline volcanic zones that may modify the stress field. Black boxes are location of figure C and D. Earthquake locations after White & Harlow (1993) for events from 1900 to 1991, and recent $M_w > 5.0$ events after the Harvard CMT catalogue. (C and D) Arc-parallel dextral shearing is suggested by the style and orientation of faults. (D) Managua fault zone with flanking weak zones, Apoyeque and Masaya volcanoes. Faults after van Wyk de Vries (1993).

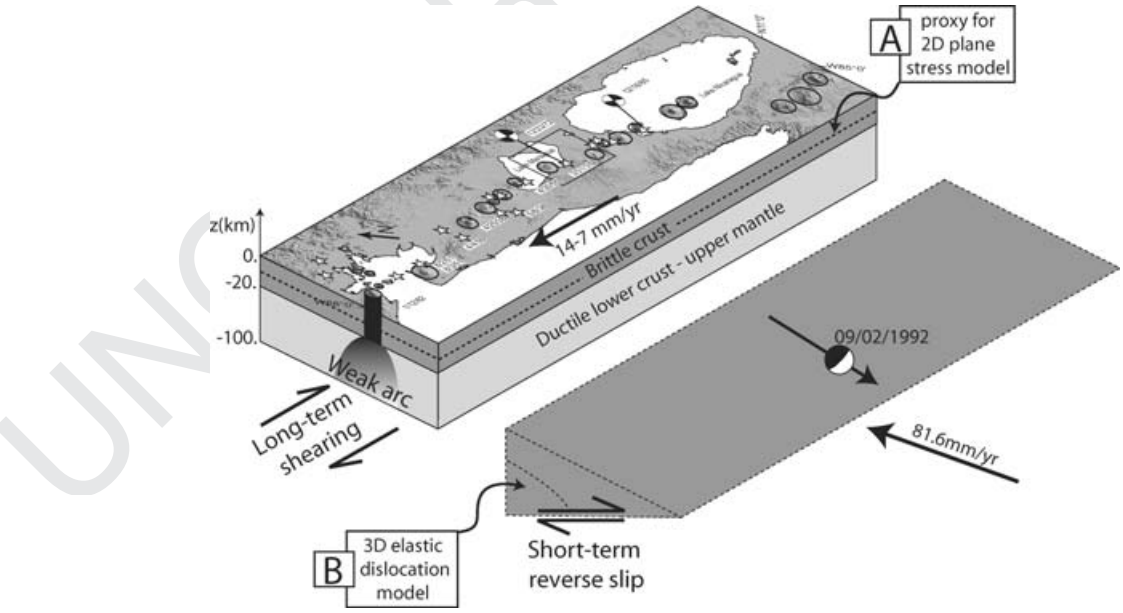

Figure 2. Mechanisms of deformation investigated in this study. In Nicaragua, oblique convergence is accommodated by slip partitioning. (A) Trench-parallel motion and long-term shearing is accommodated by slip on multiple strike-slip fault zones along the arc. We test the effects of weak zones on reactivation of N40°E sinistral faults in a 2-D plane stress model. (B) Reverse slip occurs at the subduction interface. The 1992 M_s 7.2 earthquake was the last large event on this segment of the Middle America Trench. We studied possible triggering effects on N40°E strike-slip fault zones located in the arc through 3-D elastic dislocation modelling and calculation of ΔCFS.

COLOUR FIG.

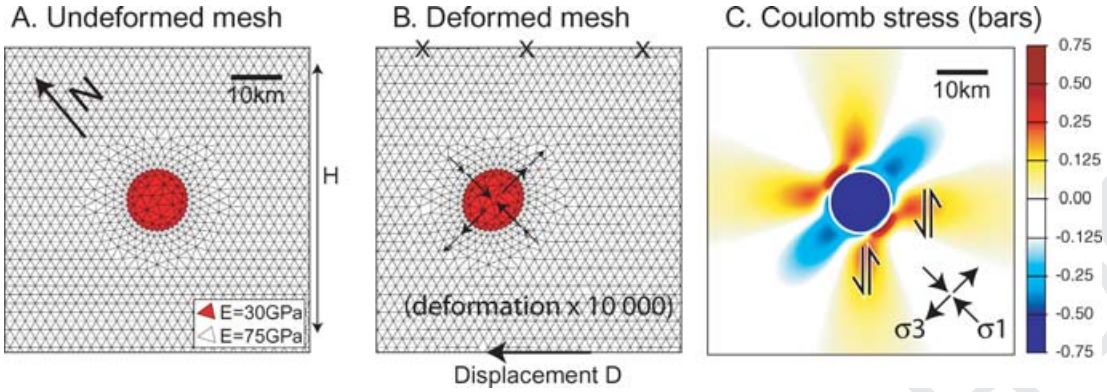

Figure 3. (A) Finite element mesh and material parameters. We study the effect of a mechanically weak zone on surrounding mechanically stronger crust under right-lateral shear. *E* is Young Modulus. Poisson's ratio is 0.25 everywhere. The mesh shown here is coarser than the model mesh for better visualization. In the models, the sides of elements are 500 m for volcanoes and 1 km for the surrounding crust. Grid boundaries (not shown) are 200 km northwest and southeast of the weak zone and 100 km northeast and southwest from the weak zone. (B) Deformed grid. The weak zone deforms more than the surrounding rock, compressing surrounding rock to the east and west and stretching to the north and south. The northeast boundary is fixed, while 1.4 m of displacement is applied to the southwest boundary. The left and right sides are free. The illustrated deformation is exaggerated by a factor of 10 000. (C) Coulomb stress changes on N40°E oriented fault planes. There are four lobes of ΔCFS with a weak zone present, where strike-slip faulting is enhanced and corresponding to the areas of differential deformation observed in b. ΔCFS in the weak zone is minimal. Thick arrows indicate the general orientations of principal stresses σ_1 and σ_3. Thin arrows represent assumed pre-existing N40°E left-lateral strike-slip faults.

a proxy for 3-D crustal stresses resulting from a deep continuous shear zone in the ductile part of the crust or upper mantle, similar to those simulated in 3-D analogue models (e.g. Tchalenko 1970; Clifton & Schlische 2001) or in 3-D elastic dislocation modelling with homogeneous material (e.g. Gomberg & Ellis 1994; Nalbant *et al.* 2002) (Fig. 2). In the following numerical models, we consider (i) 7–14 mm yr^{-1} of northwest directed forearc sliver motion, (ii) the N40°E orientation of seismogenic faults and (iii) the mechanical strength of volcanic centres. Most volcanoes along the modern arc in Nicaragua have had eruptions during Holocene time, but only eight have erupted historically (McBirney & Williams 1965; Stoiber & Carr 1973; Simkin & Siebert 1994). We follow the Global Volcanism Program guidelines and use the term 'active' for those volcanoes that erupted in the Holocene (≤10 000 yr) (Simkin & Siebert 1994). Volcanoes are generally 5–10 km in diameter (e.g. Stoiber & Carr 1973) and spacing varies from 12 to 70 km (Fig. 1b).

Mechanically weak zones within mechanically stronger crust have been shown to affect the stress field of the surrounding crust (Callot *et al.* 2002; Gudmundsson & Brenner 2003; Girard & van Wyk de Vries 2005; Li *et al.* 2005; Kaus & Podladchikov 2006). Volcanoes are known to be mechanically weak (Walker 1990) and can be considered as either highly fractured crustal material with a low Young's Modulus (e.g. Schultz 1996) or thermally weakened material with low effective viscosity (e.g. McCaffrey *et al.* 2000). We follow an approach similar to Gudmundsson & Brenner (2003), simulating volcanic centres by using a low elastic modulus, *E*. We assign the forearc, backarc and areas between the volcanoes an $E_1 = 75$ GPa, and volcanic zones an $E_2 = 30$ GPa (Fig. 3a). The ratio between E_1 and E_2 is 0.4, a realistic value based on studies analysing earthquake *b*-values and *P*- and *S*-wave velocities in volcanic terrain (e.g. Du *et al.* 1997). The Poisson's ratio υ for both materials is assumed to be 0.25. We define the horizontal extent of a weak zone to be the topographic base of the active volcano (Stoiber & Carr 1973).

In our simple elastic models, the earthquake cycle is not modelled directly, and ΔCFS increases monotonically with time. Of course, in reality, an earthquake occurs when the shear stress reaches some critical value. The maximum accumulated shear stress in our models thus depends in part on the earthquake recurrence interval, which is poorly known for Nicaraguan arc earthquakes. The 1931 and 1972 Managua earthquakes ruptured two parallel faults that are ∼2 km apart. If we assume that these faults are the manifestation of a single fault at upper crustal depth, the apparent recurrence interval would be 41 yr. An earthquake may have occurred in 1884 (Leeds 1974), changing the average recurrence interval to 44 yr. Other faults appear to have recurrence interval in excess of 100 yr. For simplicity we assume that arc earthquakes rupture individual fault segments every 100 yr, and calculate corresponding ΔCFS values.

Displacement boundary conditions are determined as follows. Studies of the deflection of earthquake slip vectors along the Middle America Trench (MAT) have estimated northwest motion of the Nicaraguan forearc at 7 ± 8 mm yr^{-1} (McCaffrey 1996) and 14 ± 2 mm yr^{-1} (DeMets 2001). Geodetic GPS studies indicate that the forearc is moving to the northwest relative to the Caribbean plate at a velocity of ∼7 mm yr^{-1} at the GPS site MANA, Managua, Nicaragua (Fig. 1a). The backarc (Nicaraguan highlands) does not move relative to the Caribbean plate within uncertainties (Lopez *et al.* 2005). We assume a 200 km wide shear zone, with a zero displacement boundary condition in the backarc, linearly increasing to 0.7 m (100 yr of shear) centred on the arc and a total of 1.4 m at the Middle America trench. The northwest and southeast boundaries remain free and are sufficiently distant to avoid boundary effects (Fig. 3). The 100-yr shear deformation equals a shear strain of about 7.e-6, that is the ratio of 1.4 m deformation over 200 km, and a shear angle or a clockwise rotation of 0.0004°.

Deformation of the weak zones causes a redistribution of stress in the surrounding crust. To study whether this affects the stress field along N40°E trending strike-slip faults, we calculate the corresponding change in CFS, following a methodology detailed in King *et al.* (1994). Studies of ΔCFS are typically used to assess whether an earthquake on a given fault changes the stress state on an adjacent segment of the same fault or a neighbouring fault, such that it either promotes ('triggers') or inhibits future earthquakes (e.g. Harris 1998). These studies, investigate short-term (i.e. days to months) ΔCFS. Here, we modify this approach to assess whether long-term (i.e. years) forearc motion, as modelled by our

displacement boundary condition, may promote failure on arc-normal faults in the presence of volcanic weak zones.

The ΔCFS on a fault depends on the change of shear stress $\Delta\sigma_s$ and change of normal stress $\Delta\sigma_n$: $\Delta \text{CFS} = |\Delta\sigma_s| - \mu' \Delta\sigma_n$, where $\mu' = 0.4$ is the effective coefficient of sliding friction that includes the effects of pore pressure (see King *et al.* 1994). Positive $\Delta\sigma_n$ is compressive and $\Delta\sigma_s$ is positive in the slip direction. The regional stress field, that is, the shear and normal stresses caused by shearing in a homogeneous material, is subtracted from the above equation to retain the sole effect of the volcanoes on N40°E striking faults. Positive ΔCFS promotes, while negative ΔCFS inhibits slip on a given fault plane.

We investigate three types of models. The first model is run with a homogeneous crustal rheology (i.e. no volcanic weak zones). In the second model, we introduce a weak zone (volcano) in the crust. In the final model, we use a realistic distribution of volcanoes in Nicaragua, southern El Salvador and northern Costa Rica. In these three models, the only source of loading is the regional northwest-directed dextral shear.

3 RESULTS

Deformation in the model domain is homogeneous without a weak zone (model 1). There is no preferential region where failure is promoted on left-lateral strike-slip faults oriented 45° clockwise relative to σ_1. However, with inclusion of a weak zone, deformation is heterogeneous (model 2; Fig. 3b). The initially circular volcano deforms, becoming elliptical, and there is differential deformation between the volcano and surrounding crust. The surrounding crust is compressed where the volcano lengthens and extends where the volcano shortens (Fig. 3b). There are four lobes of high ΔCFS around the weak zone where strike-slip earthquakes are enhanced (Fig. 3c). These lobes are located in the NE, SE, SW and NW quadrants around the weak zone. Lobes of negative ΔCFS are located east and west of the weak zone. These results are comparable to previous numerical studies on the relationship between volcanic or tectonic weak zones and active fault zones (King *et al.* 1994; Feigl *et al.* 2000; Gudmundsson & Brenner 2003).

For model 3 we find that the ΔCFS on N40°E oriented faults, after subtracting the regional stress field, shows a maximum increase between volcanoes, suggesting that arc-normal faults are encouraged to slip (Fig. 4). ΔCFS reaches a maximum of 0.6 bars between volcanoes. By varying the Young's Modulus of volcanic centres by an order of magnitude (i.e. 3 MPa), the range of ΔCFS becomes −1.6/1.6 bars in 100 yr compared to −0.6/0.6 bars with a 30 MPa Young's Modulus. All of these values are high enough to promote earthquake failure, assuming criteria used in other studies, where even values less than 0.1 bar are sometimes assumed to be sufficient to influence earthquake failure (e.g. Harris 1998; Nostro *et al.* 1998; Stein 2004). The 1931 and 1972 Managua earthquakes occurred where we calculate Coulomb stress change higher than 0.2 bars per 100 yr. We discuss the correlation of ΔCFS and earthquakes below.

4 LOCATION OF HISTORICAL EARTHQUAKES

We now compare the epicentre locations to the volcanic centres and the regions of maximum CFS changes (Table 1). Earthquake epicentre and focal mechanism locations are less than optimal for Nicaragua, making statistical comparison of our stress field to recent earthquakes difficult. For a few earthquakes we have been able to compare epicentre locations derived by inversion of teleseismic data to local earthquake relocations (e.g. LaFemina *et al.* 2002), finding differences on the order of 10–20 km. However, mapped surface ruptures and earthquake intensity maps (e.g. Carr & Stoiber 1977; White & Harlow 1993; Cowan *et al.* 2000; LaFemina *et al.* 2002), suggest that active fault zones are located in zones of positive ΔCFS. Out of 23 events, 12 earthquakes clearly correspond to positive ΔCFS (Table 1). Of these events, eight have ΔCFS higher than 0.1 bars per 100 yr. Four additional events are within 1 km of areas with positive ΔCFS. Therefore, 70 per cent of the $M_s >$ 4.5 earthquakes may be related to increasing ΔCFS caused by weak zone deformation.

Not all earthquakes here occur on N40°E trending faults. An M_s 6.0 earthquake in 1985 is thought to be located on the Ochomogo fault zone, oriented N55°E (van Wyk de Vries 1993) (Fig. 1b). The earthquake situated at the southeastern border of the modelled weak zone for Zapatera volcano likely correlates with the maximum ΔCFS increase found to the southeast (Fig. 4). A N55°E fault at the base of the volcano near the location of the 1985 earthquake has a maximum ΔCFS of 0.4 bars compared to 0.5 bars on a N40°E fault.

The age of Apoyo volcano is uncertain. Caldera eruptions are dated at about 23 000 yr Before Present but younger activity may have occurred on the flanks. When the volcano is considered as a weak zone, the earthquakes on 2000 July 6 correspond to areas where Δ CFS > 0.1 bars. When the volcano is removed, ΔCFS remains positive. Earthquakes on 1955 April 4 and on 1999 August 6 are located in zones with ΔCFS nearly zero. The proximity in space

Table 1. Relationship between earthquakes and ΔCFS due to shear deformation of volcanoes, calculated on N40°E sinistral faults along the arc from northwest to southeast. Earthquakes in white rows occurred where predicted Coulomb stress changes are positive or nearly zero, that is, within 1 km distance from areas of positive ΔCFS. Earthquakes in the dark-grey row have low magnitude and are located inside modelled weak zone. Earthquakes in light grey rows occurred in stress shadows or negative ΔCFS surrounding the volcanoes. The 1951 and 1985 events are located at the base of volcanoes. The ΔCFS may correspond to a stress shadow (1951) or a maximum (1985). If Apoyo volcano (uncertain age) is removed, the ΔCFS of the M5.0 and M5.1 events on 2000 June 7 remain greater than zero. The numbers in brackets are the number of events occurring the same day and at similar location.

Date	Ms	CFS in bars
04/03/99	4.9	>0
04/03/99	5.7	>0
02y/20/06	5.6	∼0
01/12/82	6.0	>0
08/2/51 (2)	5.8–6.0	< −0.3/> −0.2
04/04/55	6.2	∼0
8/31/84	5.4	>0.1
04/25/38	5.9	>0
05/06/38	6.1	> −0.1
08/05/99 (3)	4.6/4.5/4.6	< −0.3
08/06/99	4.6	∼0
04/30/55	6.0	>0.4
03/31/31	6.0	>0.2
12/23/72	6.2	>0.2
07/08/00	4.7	> −0.2
07/06/00	5.1	>0.4/>0
07/06/00	5.0	>0.1/>0.1
12/16/85	6.0	< −0.3/>0.5
08/03/05	5.3	>0.4
08/03/05	6.0	>0.1

COLOUR FIG.

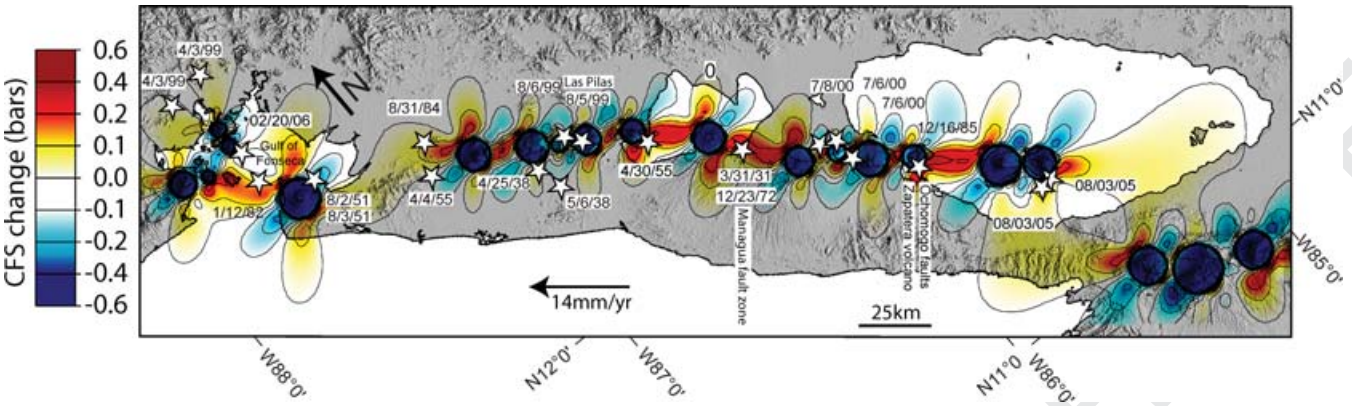

Figure 4. Coulomb stress changes on N40°E oriented left-lateral fault planes in Nicaragua, showing maximum between volcanoes and minimum at volcanoes. The shear and normal stresses caused by regional shearing without a weak zone are 1.5 and 0 bars. The contour interval is 0.1 bars.

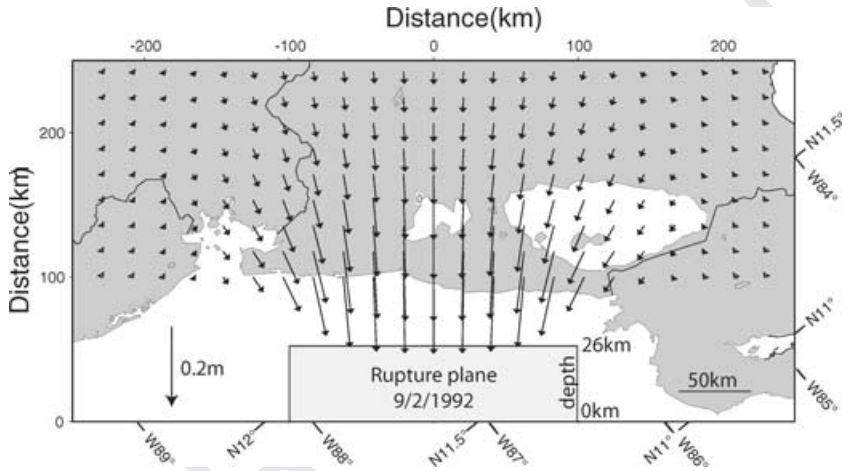

Figure 5. Displacement field resulting from the 1992 subduction earthquake. The rectangle indicates the slipping patch, 200 km long and 100 km wide with a 15° fault dip and 0.5 m slip inferred from the aftershocks (Ide *et al.* 1993).

and time of the latter event to two earlier earthquakes and an eruption suggest that it may have been triggered (LaFemina *et al.* 2004). For the three synchronous 1999 August 5 events at Cerro Negro, the modelled broad weak zone may not well reproduce the complexity of the Las Pilas edifice (LaFemina *et al.* 2004) (Fig. 1c). Furthermore, these earthquakes were of lower magnitude than previously considered as destructive. Earthquakes in 1951 near the Gulf of Fonseca and on 2000 August 7 north of Apoyo were located in stress shadows or areas of negative ΔCFS. Perhaps stresses take longer to build on these fault zones; the rate of seismicity or the number of earthquakes per time may be lower (Dieterich 1994; Harris 1998; Stein 2003). Finally, because NW-trending dextral strike-slip faults and NE-trending sinistral faults are conjugates in a regional stress field that has a maximum compressive stress oriented north–south, we note that either trend may be enhanced by ΔCFS.

5 SLIP AT THE SUBDUCTION INTERFACE

Is the magnitude of ΔCFS we calculate for the volcanic arc significant compared to other processes that may affect fault stress? To test this, we compare the magnitude of ΔCFS from our previous models (i.e. regional shear with volcanic weak zones) to the effect exerted by the 1992 September 2 M_s 7.2 subduction earthquake (Fig. 2). This is the largest subduction zone earthquake along the Nicaragua segment of the Middle America Trench that is well recorded and studied. We use the program POLY3D (Thomas 1993) to develop elastic dislocation models for this event, calculating the resultant ΔCFS at 10 km depth on trench-normal N40°E sinistral faults (Fig. 6). Ide *et al.* (1993) used the distribution of aftershocks following the 1992 event to determine the geometry of the fault plane, obtaining a plane with 200 km along strike length, 100 km downdip width and dipping at 15° (Fig. 5). This model requires 0.5 m of slip (Ide *et al.* 1993). For the ΔCFS calculations presented here, Poisson's ratio is assumed to be 0.25 and the Young Modulus 75 GPa as in the previous models of weak volcanic zones.

Subduction earthquakes with slip perpendicular to the trench may unclamp trench-parallel strike-slip faults in the arc, enhancing their propensity for slip (ten Brink & Lin 2004). In contrast, changes in normal stress are minimal on trench-normal faults and reactivation, if it occurs, is caused by an increase in shear stress. An antisymmetry in ΔCFS field is observed along the arc. ΔCFS is positive in the volcanic arc segment southeast of the Managua graben but negative in the northwest segment (Fig. 6). Although NE-striking faults are pervasive in the forearc, arc and backarc (e.g. Carr & Stoiber 1977; Weinberg 1992), no active fault zones are known in the forearc offshore, even though ΔCFS exceeds 0.3 bars there. This is consistent with the idea that deformation of the volcanoes is controlling fault activity. Positive ΔCFS from the subduction zone earthquakes is as

Q1
Q2

COLOUR FIG.

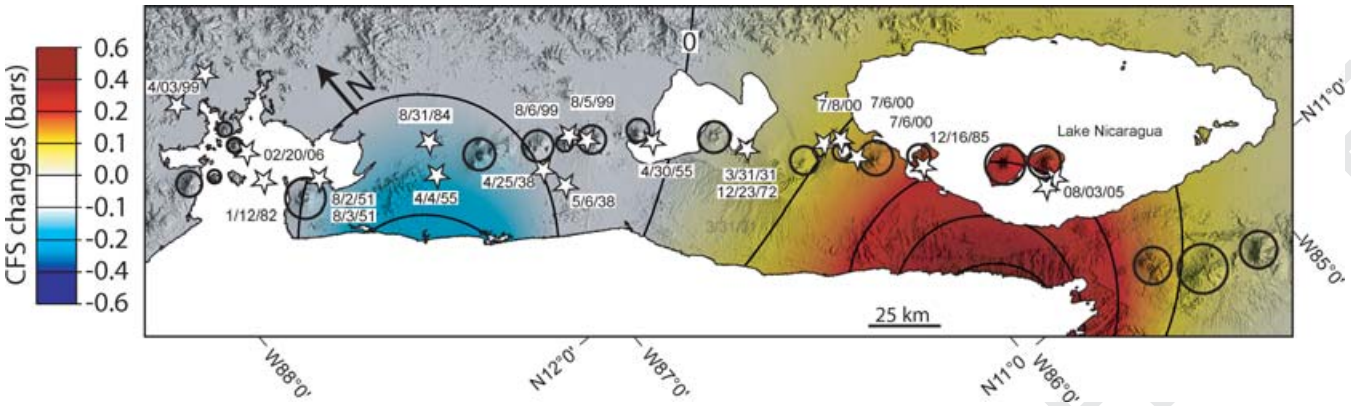

Figure 6. Coulomb stress changes ΔCFS caused by the 1992 subduction event calculated on N40°E left-lateral strike-slip faults at 10 km depth and compared with earthquakes in Nicaragua. Contour interval is 0.1 bars. Compared to the model of volcano shear deformation (Fig. 4), the pattern of ΔCFS from coseismic deformation is significantly different. However the magnitude of ΔCFS is similar. After the 1992 thrust event, five earthquakes occurred 8–13 yr later in the southeast, in areas with less than 0.3 bars predicted ΔCFS. The northwest segment experienced seven earthquakes in 1999 and 2006, in areas with predicted negative ΔCFS.

high as 0.3 bars within 20 km of the arc, less than the 0.6 bars calculated in our 2-D plane stress models with 100-yr volcanic shear deformation. Thus, the presence of weak volcanic centres does appear to exert significant control on the stress field compared to other large sources of stress change.

Following the 1992 earthquake, five earthquakes were located in the southeast arc segment, a region where our subduction model predicts less than 0.3 bars positive ΔCFS. The relevant process, that is, volcano shear model or subduction earthquake model, cannot be discriminated for the 200 July 6 or 2005 August 3 events, because ΔCFS > 0 in both models. The 2000 July 8 event is located in an area of negative ΔCFS by shear deformation, and hence may be related to subduction coseismic deformation. The 8 yr delay between the 1992 earthquake and the subsequent event may reflect the influence of post-seismic viscous flow in the lower crust or upper mantle, unaccounted for in our simple models. The 2000 July 8 event may have been triggered by the two earlier and nearby events on 200 July 6 as well. The northwest segment was the location of six earthquakes in 1999 and one earthquake in 2006 (Fig. 6; Table 1). The 1999 and 2006 events could not be triggered by the 1992 subduction earthquake as they are all located in an area of negative ΔCFS. In contrast, all events except the 1999 August 5 events correspond to positive ΔCFS in our weak zone model and hence may be attributed to enhanced stress by volcano deformation.

6 DISCUSSION

Forearc sliver transport and corresponding shear deformation are key aspects of the long-term tectonics in and near the volcanic arc of Nicaragua. Our models suggest that weak volcanic centres have a significant effect on the stress state of nearby faults. The long-term deformation of volcanic weak zones may explain the tendency for faults between volcanoes to slip.

We used the theory of Coulomb failure stress to study this process. This theory explains fault reactivation in general (Byerlee 1978) and has been widely applied to earthquake triggering studies, for example, an earthquake caused by a stress change from a neighbouring earthquake or filling of a nearby water reservoir, (e.g. King *et al.* 1994; Harris 1998). The difference between these two applications is that ΔCFS resulting from forearc deformation builds up slowly and steadily until released by earthquakes. The maximum ΔCFS suggested by our models is ≤0.6 bars 100 yr−1, similar to values estimated in earthquake triggering studies (Stein 1999). Stress magnitudes may change if other parameter values, for example, shear zone width or rate, volcano diameter, and/or rheology are assumed. However, the general pattern of stress increase between two volcanic centres is clear.

With the understanding that volcanic centres can be considered as crustal weak zones, we are confident that this analysis is applicable not only to Nicaragua but also to other volcanic regions of the world. Our models give a first order estimate of the effects of volcanic weak zones on stress distribution in the surrounding crust. Other deformation processes may also influence the stress conditions between volcanoes, such as gravitational loading and magmatic deformation of volcanic edifices (van Wyk de Vries & Merle 1998) or the interaction with nearby tectonic or magmatic events, which may explain temporal and spatial clustering of earthquakes such as the 1951 or 1999 events (Nostro *et al.* 1998; Diez *et al.* 2005).

Q3

7 SUMMARY

Long term ΔCFS in the upper plate of subduction zones caused by deformation of volcanically modified crust in a stress field dominated by regional shear may be as important as short-term stress changes resulting from large subduction zone earthquakes. The reduced mechanical strength of volcanic centres leads to lower stress accumulation inside the volcanoes, and stress transfer to stronger crust between volcanic centres. Earthquakes are encouraged on faults located between active volcanic centres and oriented normal to the volcanic arc.

ACKNOWLEDGMENTS

This study was supported by grants from NASA & ONR to T.H.D and by a stipend from ''Deutsche Forschungsgemeinschaft DFG'' to B.C. (CA459-1). Careful reviews by Thora Árnadóttir, Susan Ellis and John Beavan improved the manuscript. The program POLY3D was developed by Andy Thomas and made available by Stanford. Thanks also to Jay Melosh for free access to his program TEKTON.

REFERENCES

Byerlee, J.D., 1978. Friction of Rocks, *Pure Appl. Geophys.*, **116**, 615–626.

Callot, J., Geoffroy, L. & Brun, J., 2002. Development of volcanic passive margins: Three-dimensional laboratory models, *Tectonics*, **21**(6), 1052, doi:10.1029/2001TC901019.

Carr, M.J. & Stoiber, R.E., 1977. Geologic setting of some destructive earthquakes in Central America, *Geol. Soc. Am. Bull.*, **88**, 151–156.

Clifton, A.E. & Schlische, R.W., 2001. Nucleation, growth, and linkage of faults in oblique rift zones: Results from experimental clay models and implications for maximum fault size, *Geology*, **29**(5), 455–458.

Cowan, H., Machette, M.N., Amador, X., Morgan, K.S., Dart, R.L. & Bradley, L.A., 2000. Map and database of quaternary faults in the vicinity of Managua, Nicaragua. U.S. Geological Survey Open-File Report 00–0437.

DeMets, C., 2001. A new estimate for Cocos-Caribbean plate motion: implications for slip along the Central American volcanic arc, *Geophys. Res. Lett.*, **28**, 4043–4046.

Díez, M., La Femina, P.C., Connor, C.B., Strauch, W. & Tenorio, V., 2005. Evidence for static stress changes triggering the 1999 eruption of Cerro Negro Volcano, Nicaragua and regional aftershock sequences, *Geophys. Res. Lett.*, **32**, L04309, doi:10.1029/2004GL021788.

Dieterich, J.H., 1994. A constitutive law for rate of earthquake production and its application to earthquake clustering, *J. Geophys. Res.*, **99**, 2601–2618.

Du, Y., Segall, P. & Gao, H., 1997. Quasi-static dislocations in three dimensional inhomogeneous media, *Geophys. Res. Lett.*, **24**(18), 2347–2350, doi:10.1029/97GL02341.

Feigl, K.L., Gasperi, J., Sigmundsson, F. & Rigo, A., 2000. Crustal deformation near Hengill volcano, Iceland, 1993–1998: Coupling between magmatic activity and faulting inferred from elastic modelling of satellite radar interferograms, *J. Geophys. Res.*, **105**(B11), 25 655–25 670.

Girard, G. & van Wyk de Vries, B., 2005. The Managua Graben and Las Sierras-Masaya volcanic complex (Nicaragua); pull-apart localization by an intrusive complex: results from analogue modeling, *J. Volc. Geotherm. Res.*, **144**, 37–57.

Gomberg, J. & Ellis, M., 1994. Topography and tectonics of the central New Madrid seismic zone: Results of numerical experiments using a three-dimensional boundary element program, *J. Geophys. Res.*, **99**(B10), 20 299–20 310, doi:10.1029/94JB00039.

Gudmundsson, A. & Brenner, S.L., 2003. Loading of a seismic zone to failure deforms nearby volcanoes: a new earthquake precursor, *Terra Nova*, doi:10.1046/j.1365-3121.2003.00481.x, 187–193.

Harris, R.A., 1998. Introduction to special section: Stress triggers, stress shadows and implications for seismic hazard, *J. Geophys. Res.*, **100**, 12 985–13 005.

Ide, S., Imamura, F., Yoshida, Y. & Abe, K., 1993. Source characteristics of the Nicaraguan tsunami earthquake of September 2, 1992, *Geophys. Res. Lett.*, **20**(9), 863–866, doi:10.1029/93GL00683.

Kaus, B.J.P. & Podladchikov, Y.Y., 2006. Initiation of localized shear zones in viscoelastoplastic rocks, *J. Geophys. Res.*, **111**, B04412, doi:10.1029/2005JB003652.

King, G.C.P., Stein, R.S. & Lin J., 1994. Static stress changes and the triggering of earthquakes, *Bull. Seismol. Soc. Amer.*, **84**, 935–953.

LaFemina, P.C., Dixon, T.H. & Strauch, W., 2002. Bookshelf faulting in Nicaragua, *Geology*, **30**, 751–754.

LaFemina, P.C., Connor, C.B., Hill, B.E., Strauch, W. & Armando Saballos, J., 2004. Magma-tectonic interactions in Nicaragua: the 1999 seismic swarm and eruption of Cerro Negro volcano, *J. Volcanol. Geotherm. Res.*, **137**, 187–199.

Leeds, J., 1974. Catalog of Nicaragua earthquakes, *Bull. Seis. Soc. Amer.*, **64**(4), 1135–1158.

Li, Q., Liu, M. & Sandvol, E., 2005. Stress evolution following the 1811–1812 large earthquakes in the New Madrid Seismic Zone, *Geophys. Res. Lett.*, **32**, L11310, doi:10.1029/2004GL022133.

Lopez, A.M., Stein, S., Dixon, T., Sella, G., Calais, E., Jansma, P., Weber, J. & LaFemina, P., 2006. Is there a northern Lesser Antilles forearc block?, *Geophys. Res. Lett.*, **33**, doi:10.1029/2005GL025293.

McBirney, A.R. & Williams, H., 1965. Volcanic history of Nicaragua, *University of California Publications in Geological Sciences*, **55**, 65.

McCaffrey, R., Zwick, P., Bock, Y., Prawirodirdjo, L., Genrich, J., Stevens, C., Puntodewo, S. & Subarya, C., 2000. Strain partitioning during oblique plate convergence in northern Sumatra: Geodetic and seismologic constraints and numerical modeling, *J. Geophys. Res.*, **105**, 28 363–28 376.

McCaffrey, R., 1996. Estimates of modern arc-parallel strain rates in fore arcs, *Geology*, **24**(1), 27–30.

Melosh, H.J. & Raefsky, A., 1980. The dynamic origin of subduction zone topography, *J. Geophys. J.R. Astron. Soc.*, **60**, 33–354.

Nalbant, S.S., McCloskey, J., Steacy, S. & Barka, A.A., 2002. Stress accumulation and increased seismic risk in eastern Turkey, *Earth planet. Sci. Lett.*, **195**, 291–298.

Nostro, C., Stein, R.S., Cocco, M., Belardinelli, M.E. & Marzocchi, W., 1998. Two-way coupling between Vesuvius eruptions and southern Apennine earthquakes, Italy, by elastic stress transfer, *J. Geophys. Res.*, **103**(B10), 24 487–24 504.

Rydelek, P.A. & Sacks, I.S., 1990. Asthenospheric viscosity and stress diffusion: a mechanism to explain correlated earthquakes and surface deformation in NE Japan, *Geophys. J. Int.*, **100**, 39–58.

Schultz, R.A., 1996. Relative scale and the strength and deformability of rock masses, *J. Struct. Geol.*, **18**(9), 1139–1149.

Simkin, T. & Siebert, L., 1994. *Volcanoes of the world; a regional directory, gazetteer, and chronology of volcanism during the last 10 000 yr*, Geoscience Press, Tucson, AZ, United States (USA).

Stein, R.S., 1999. The role of stress transfer in earthquake occurrence, *Nature*, **402**, 605–609.

Stein, R.S., 2004. Tidal triggering caught in the act (Perspective), *Science*, **305**, 1248–1249.

Stein, R.S., 2003. Earthquake conversations, *Scientif. Am.*, **288**, 72–79.

Stoiber, R.E. & Carr, M.J., 1973. Quaternary volcanic and tectonic segmentation of Central America, *Bull. Volcanol.*, **37**, 304–325.

Tchalenko, J.S., 1970. Similarities between shear zones of different magnitudes, *Geol. Seismol. Soc. Amer.*, **81**, 1625–1640.

ten Brink, U. & Lin, J., 2004. Stress interaction between subduction earthquakes and forearc strike-slip faults: modeling and application to the northern Caribbean plate boundary, *J. Geophys. Res.*, **109**, B12310, doi:10.1029/2004JB003031.

Thomas, A.L., 1993. Poly3D: a three-dimensional, polygonal element, displacement discontinuity boundary element computer program with applications to fractures, faults, and cavities in the earth's crust. *M.S. thesis*, Stanford University, Stanford, California, 221p.

van Wyk de Vries, B., 1993. Tectonic and magma evolution of Nicaragua Volcanic Systems, *PhD. thesis*, The Open University, England.

van Wyk de Vries, B. & Merle, O., 1998. Extension induced by volcanic loading in regional strike-slip zones, *Geology*, **26**, 983–986.

Walker, G.P.L., 1990. Geology and volcanology of the Hawaiian Islands, *Pacific Sci.*, **44**, 315–347.

White, R.A. & Harlow, D.H., 1993. Destructive upper-crustal earthquakes of Central America since 1900, *Seismol. Soc. Am. Bull.*, **38**, 1115–1142.

QUERIES

Journal: GJI
Paper: gji3353

Dear Author

During the copy-editing of your paper, the following queries arose. Please respond to these by marking up your proofs with the necessary changes/additions. Please write your answers on the query sheet if there is insufficient space on the page proofs. Please write clearly and follow the conventions shown on the corrections sheet. If returning the proof by fax do not write too close to the paper's edge. Please remember that illegible mark-ups may delay publication.

Query Reference	Query	Remarks
Q1	Au: Reference Carr & Stoiber (1977) is not present in the reference list. Please check.	
Q2	Au: Reference Weinberg (1992) is not present in the reference list. Please check.	
Q3	Au: Reference Diez *et al.* (2005) is not present in the reference list. Please check.	
Q4	Au: Reference Díez *et al.* (2005) is not cited in text. Please check.	
Q5	Au: Reference Lopez *et al.* (2006) is not cited in text. Please check.	

MARKED PROOF

Please correct and return this set

Please use the proof correction marks shown below for all alterations and corrections. If you wish to return your proof by fax you should ensure that all amendments are written clearly in dark ink and are made well within the page margins.

Instruction to printer	*Textual mark*	*Marginal mark*
Leave unchanged	··· under matter to remain	New matter followed by or or
Insert in text the matter indicated in the margin		
Delete	through single character, rule or underline or through all characters to be deleted	or
Substitute character or substitute part of one or more word(s)	through letter or through characters	new character or new characters
Change to italics	under matter to be changed	
Change to capitals	under matter to be changed	
Change to small capitals	under matter to be changed	
Change to bold type	under matter to be changed	
Change to bold italic	under matter to be changed	
Change to lower case	Encircle matter to be changed	
Change italic to upright type	(As above)	
Change bold to non-bold type	(As above)	
Insert 'superior' character	through character or where required	or under character e.g. or
Insert 'inferior' character	(As above)	over character e.g.
Insert full stop	(As above)	
Insert comma	(As above)	
Insert single quotation marks	(As above)	or and/or or
Insert double quotation marks	(As above)	or and/or or
Insert hyphen	(As above)	
Start new paragraph		
No new paragraph		
Transpose		
Close up	linking characters	
Insert or substitute space between characters or words	through character or where required	
Reduce space between characters or words	between characters or words affected	